Age And Speleogenesis Of Gypsum Caves In Emilia-Romagna (N Italy)

Andrea Columbu[1,1], Veronica Chiarini[2,3], Jo De Waele[2], Russell Drysdale[1,3], Jon Woodhead[4], John Hellstrom[4] and Paolo Forti[2]

Affiliation: [1]*School of Geography, University of Melbourne (Australia), University of Melbourne, 221 Bouverie street, 3010, Melbourne, Australia acolumbu@student.unimelb.edu.au andrea.columbu2@unibo.it rnd@unimelb.edu.au*
[2]*Department of Biological, Geological and Environmental Sciences, University of Bologna, Via Zamboni 67, 40127 Bologna, Italy vero.ch88@hotmail.it jo.dewaele@unibo.it paolo.forti@unibo.it*
[3]*University of Savoie, Laboratoire EDYTEM, bd de la Mer Caspienne, Le Bourget du Lac cedex, F-73376, France*
[4]*School of Earth Sciences, University of Melbourne, Corner Swanston & Elgin streets, 3010, Melbourne, Australia jdwood@unimelb.edu.au j.hellstrom@unimelb.edu.au*

Abstract

More than 600 caves have been surveyed in the Triassic and Messinian gypsum beds of the Northern Apennines (Emilia-Romagna region, N Italy). Despite the fact that these caves have been studied for a very long time, their age was inaccurately believed to be Late Glacial. In fact, the fast dissolution of gypsum and the regional uplift of the mountain chain lead to the belief that speleogenesis could have started only recently.

Dating of the infilling sediments can assess a minimum age of the cave passages. U-Th dating of carbonate speleothems sampled in these gypsum caves has been carried out in several karst areas in the region. The results show that caves started forming at least ~600 kyrs ago, and that caves were mainly carved during relatively cold climate stages, when rivers formed terraces at the surface and aggradation caused paragenesis in the stable and active cave levels. The carbonate speleothems, on the other hand, mainly formed during warm and wet intervals.

Keywords: U/Th dating; carbonate speleothems; evaporite karst; Middle Pleistocene; Paleoclimate

1. Introduction

Messinian gypsum outcropping in Emilia Romagna (North Italy) hosts more than 600 caves (De Waele *et al.* 2011). In this area, speleogenesis was inaccurately assigned to the Late Pleistocene-Holocene, with peaks during the late glacial (Demaria 2002; Forti 2003; Pasini 2012). Scarce radiometric ages (Forti and Chiesi 2001; Forti 2003), archeological (Miari 2007; Negrini 2007) and paleontological (Pasini 1969) findings sustained this idea. Speleogenesis in gypsum can occur up to hundred times faster than in carbonates (Klimchouk 2000); at the same time, the high solubility of gypsum makes the surface outcrops subjected to intense karst denudation, which can lead to the demolition of the underground cave systems. These are the main reasons why the age of the currently explorable caves, hence the inception of speleogenesis, has been underestimated. Establishing the age of a cave is not an easy task (Sasowsky 1998), especially in the cases where direct approaches, as dating speleogenetic byproducts (Polyak *et al.* 1998, 2016; Plan *et al.* 2012), are inapplicable. Thus, ages are most of the time estimated by dating cave infilling sediments (Audra *et al.* 2006), such as speleothems, fossils, artefacts, etc.. However, even with this methodology the age of speleogenesis could considerably be miscalculated, if dated materials are much younger than cave carving processes. Besides radiometric dating, cave evolutionary models should be sustained by geological, paleoclimatic and paleo-environmental considerations, in order to procure a truly reliable timing for karst processes.

We studied a dozen caves belonging to five different karst systems carved in the Emilia Romagna gypsum areas by dating, using the U-Th method, twenty carbonate speleothems. Radiometric ages were then used to build a solid karst evolutionary model, in turn anchored to previously dated local geological events and the connection between climate cycles and speleogenesis (Columbu *et al.* 2015). This model, besides allowing to precisely estimate the age of speleogenesis in this portion of the Apennine chain, may also be applied to other gypsum karst areas having similar geological and climatic conditions.

2. Area of study, material and methods

Messinian gypsum in Emilia Romagna region belongs to the *Vena del Gesso* Formation (Vai and Martini 2001; Lugli *et al*, 2010), outcropping with well-recognisable cuesta-like morphologies. The formation is infrequently overlain by marine silt and clays (*Argille Azzurre* Fm. - Amorosi *et al.* 1998), littoral sandstones (*Sabbie Gialle* Fm. - Cyr and Granger 2008) and continental sediments (continental Quaternary - Amorosi *et al.* 2015). The explored caves and relative samples are (bracketed IDs refer to speleothems sampled in the quoted cave or in the area of the cave entrance – Fig. 1 for some examples): Abisso Mezzano (RT), 3 Anelli (3A), Abisso 50 (A50), Pozzo Pollini (PP), Grotta Oliver (GO) and Galleria Principale caves (RTy) in the Re Tiberio – Monte Tondo system; Spipola cave (SpD, Sp1, and SpS) in the Spipola-Acquafredda system; Peroni (P2 and P3) and Mornig (Mor2) caves in the Castelnuovo system; Rio Basino (RBT, RB1, and RB3) cave in the Rio Stella-Rio Basino system; Monte Mauro (MM2 and MM4) and Banditi (Ba1.1, Ba2.1 and BaBig) caves in the Monte Mauro system. All are epigenic caves, sub-horizontal in section; karst systems report stacked-like juxtaposition of these multi-level sub-horizontal passages. Their formation is

Figure 1. Calcite speleothems of the Emilia Romagna gypsum caves. A) The active flowstone forming on the riverbed of Rio Basino (photo Piero Lucci); B) A50 flowstone of Abisso 50, grown around 76 ka (MIS5a); C. The Banditi flowstone (a portion of BaBig) which grew during isotope stage MIS5e (photo Jo De Waele); D. One of the Monte Mauro flowstones (MM2) found in the forest, with the gypsum cave immediately dissolved but calcite flowstone preserved. This flowstone appears to have grown in two distinct periods somewhere between 240 and 320 kyrs ago (comprising both MIS9 and MIS7); E. Active flowstone in the Mornig cave (photo Francesco Grazioli).

linked to the lowering and stabilization of the local base level (i.e. rivers) (Columbu *et al*. 2015), considering that the rapid uplifting affecting the area triggers the incision of the Northern Apennines flank valleys. Speleothems are mostly calcite flowstones, and only three calcite stalagmites were sampled (BaBig, Mor2, SpS). Top and bottom of each speleothem was dated with the U-Th methodology; for the tallest speleothems, age constraints were improved by several internal dates. U-Th is the more widely used methodology for dating carbonate speleothems (Richards and Dorale 2003). Preparation of subsamples for dating, mass spectrometer setting and statistical treatment of the final data strictly followed the protocols in force at the University of Melbourne – School of Earth Sciences, reported elsewhere in detail (Hellstrom 2003, 2006; Drysdale et al. 2009, 2012).

3. Results, discussion and final remarks

U-Th results are shown in Table 1; all speleothems grew during periods of relative warm and wet climate (Fig. 2) considering the last ~800 kyrs (Columbu *et al*. 2017). Conversely, sub-horizontal cave tunnels formed mostly during stages of relative cold and dry climates (Columbu *et al*. 2015). In fact, cave level altitudes correlate with strath river terraces that, in

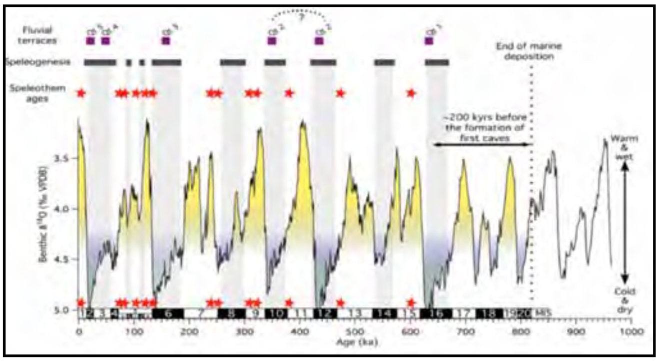

Figure 2. Speleogenetic processes over the last ~800 ka. Stars indicate the basal ages of the studied speleothems (except for the sample Ba2 at ~380 ka, which reported only the top age; Holocenic ages are aggregated in a single star). The ages mainly fit with periods of warm and wet climate (yellow shading). The formation of the different cave levels (rectangles) is correlated with the cold-dry climate stage (gray shading) that occurred before the warm-wet period indicated by the age of the speleothems (see figure 3 and text), simultaneous with the deposition of most of the fluvial terrace sediments along the main river of the area (squares) (Cyr and Granger 2008; Picotti and Pazzaglia 2008; Wegmann and Pazzaglia 2009). The climatic curve (and MIS subdivision) refers to the δ18O benthic stack of Lisiecki and Raymo (2005). First caves were carved at least ~630 kyrs ago, 200 kyrs after the retreat of the Adriatic Sea.

the area of study, were all formed mostly during glaciation peaks (Cyr and Granger 2008; Picotti and Pazzaglia 2008; Wegmann and Pazzaglia 2009) (Fig. 3). An epigenic sub-horizontal cave tunnel is excavated parallel to the piezometric level at the same altitude as the base level (Fig. 3). During periods of climate deterioration, vegetation on the valley slopes is scarce, meaning that a high quantity of regolith is produced and available. Loose sediments are gravitationally conveyed toward the valley bottoms forming the terrace deposits. River terraces testify periods of stability in the paleo base level longer than 1,000 years (Wegmann and Pazzaglia 2009). This time-span is sufficiently long for the excavation of the epigenic sub-horizontal caves (Columbu *et al*. 2015), which operate as through-flow channels (Klimchouk 2000) transporting water from the sinking points (i.e. dolines or blind valleys) to the resurgences. During the following warm-wet period vegetation abounds, increasing the level of CO_2 in the soils. At the same time, cave carving proceeds slowly and tunnels previously formed are entrenched. These appear to be ideal environmental conditions for the formation of carbonate speleothems (Columbu *et al*. 2015) (Fig. 3). At the end of warm periods, the stability of base levels terminates and valleys, as well as fluvial terraces deposits, are incised. Gypsum karst systems react to the new hydrological situation by excavating deep and narrow vertical shafts, as the 30 m deep one visible in Monte Tondo (De Waele *et al*. 2013) (Fig. 3). Once base level gets stable at a new (lower) altitudinal position, another sub-horizontal cave passage is excavated, and the cyclical above-described speleogenetic process can start all over again.

Following the previous discussion, we used the U-Th speleothems' ages as temporal reference to establish the age of speleogenesis (Fig. 2). Cave formation is assigned to the first cold period before the warm stage that allowed the deposition of speleothems (Figs. 2 and 3). Major caves formed during marine isotopic stage (MIS) 14, 12, 10, 8, 6, 3, 2 and 1, but

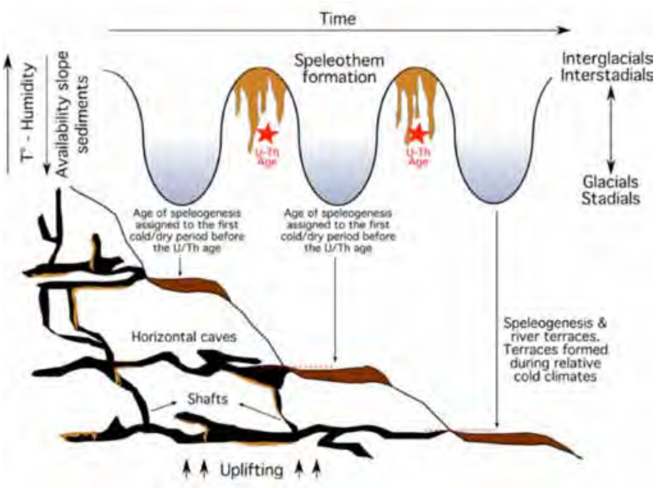

Figure 3. Schematic model of the formation of sub-horizontal cave levels and fluvial terraces in relation to cyclic climate changes. River terraces, formed during cold climates, record periods of stability in the paleo base level longer than 1,000 years (Wegmann and Pazzaglia 2009). Contemporaneously, sub-horizontal cave tunnels are carved at the same altitude. The oldest generation of speleothems in a certain cave level were deposited when the newly born cave reached a vadose status, during periods of relatively warm climates. The first cold period before the warm stage indicated by the speleothems is considered as the minimal age for the formation of the caves.

also during the glacial-like climate pulsations MIS5d and 5b (Fig. 2). The oldest speleothems in our collection provide a basal age of >580 ka (Ba1) and 468.00 $^{+130}/_{-42}$ ka (MM4 flowstone). This suggests that caves already existed in the area at least since MIS15 (i.e. ~600 kyrs ago, testified by Ba1 age and the oldest possible MM4 age). Assigning the timing of speleogenesis to the coldest period just before MIS15 (MIS16), the excavation of the first caves likely occurred at least 630 kyrs ago. It could be argued that speleogenesis might have occurred even before, but speleothems representing that age were not sampled/analysed. Furthermore, geological and geomorphological considerations make this hypothesis unrealistic. In fact, the top age of the Sabbie Gialle Fm. (the terminal marine sequence covering the gypsum) is attested at 780-820 ka (= ~800 ka) (Falgueres 2003; Muttoni *et al.* 2011). Thus, the area was submerged at least until ~800 ka, a condition that made the formation of epigenic gypsum caves impossible. These epigenic caves could only have formed when the karstifiable aquifer was unconfined, meaning that the majority of sediments overlying the gypsum were removed before the inception of the first speleogenetic events. Moreover, these cave systems need a mature hydrological network at the surface able to efficiently convey water into the underground (i.e. formation of sinkholes, protovalleys, etc.). 200,000 years (i.e. from ~800 ka to ~630 ka) is considered a sufficient and reasonable timespan to permit the dismantling of most marine sediments covering the gypsum beds and for the creation of an efficient hydrological surface drainage network (Columbu *et al.* 2017).

With these new data, we sensibly reviewed the age of speleogenesis in the Northern Italian gypsum terrains, procuring solid geochronological and geomorphological evidences. In parallel, we established an evolutionary speleological model based on the cyclical dualism between speleothems being formed during relative wet and warm climate stages and main sub-horizontal caves being carved during periods of relative dry and cold climate stages. This model may also be applied to other gypsum karst areas having similar geological and climatic conditions, which would be useful for refining the timing of other gypsum karst systems.

References

Amorosi A, Caporale L, Cibin U, Colalongo M, Pasini G, Ricci Lucchi F, Severi P, Vaiani S, 1998. The Pleistocene littoral deposits (Imola Sands) of the northern Apennines foothills. *Giornale di Geologia*, **60**, 83-118.

Amorosi A, Maselli V, Trincardi F, 2015. Onshore to offshore anatomy of a late Quaternary source-to-sink system (Po Plain–Adriatic Sea, Italy). *Earth-Science Reviews*, **153**, 212-237.

Audra P, Bini A, Gabrovšek F, Häuselmann P, Hobléa F, Jeannin P-Y, Kunaver J, Monbaron M, Šušteršić F, Tognini P, 2006. Cave genesis in the Alps between the Miocene and today: a review. *Zeitschrift für Geomorphologie*, **50**(2), 153-176.

Cheng H, Lawrence Edwards R, Shen CC, Polyak VJ, Asmerom Y, Woodhead J, Hellstrom J, Wang Y, Kong X, Spötl C, Wang X, Calvin Alexander E, 2013. Improvements in 230Th dating, 230Th and 234U half-life values, and U-Th isotopic measurements by multi-collector inductively coupled plasma mass spectrometry. *Earth and Planetary Science Letters*, **371-372**, 82-91.

Columbu A, Chiarini V, De Waele J, Drysdale RN, Woodhead J, Hellstrom J, Forti P, E, 2017. Late quaternary speleogenesis and landscape evolution in the northern Apennine evaporite areas. *Earth Surface Processes and Landforms*, in print.

Columbu A, De Waele J, Forti P, Montagna P, Picotti V, Pons-Branchu E, Hellstrom J, Bajo P, Drysdale RN, 2015. Gypsum caves as indicators of climate-driven river incision and aggradation in a rapidly uplifting region. *Geology*, **43**(6), 539-542.

Cyr AJ, Granger DE, 2008. Dynamic equilibrium among erosion, river incision, and coastal uplift in the northern and central Apennines, Italy. *Geology*, **36**(2), 103-106.

Demaria D, 2002. Emilia Romagna. In: G Madonia and P Forti (Eds.). Le aree carsiche gessose d'Italia. *Memorie dell'Istituto Italiano di Speleologia*, **2**(14), pp. 159-184.

De Waele J, Forti P, Rossi A, 2011. Il carsismo nelle evaporiti dell'Emilia Romagna. In: P Lucci and A Rossi (Eds.). *Speleologia e geositi carsici in Emilia Romagna, Pitagora, Bologna*, pp. 25-59.

De Waele J., Fabbri F., Forti P., Lucci P., Marabini S., 2013. Evoluzione speleogenetica del sistema carsico del Re Tiberio (Vena del Gesso Romagnola). In: M. Ercolani, P. Lucci, S. Piastra and B. Sansavini (Eds.). I Gessi e la Cave i Monte Tondo. Studio multidisciplinare di un'area carsica nella Vena del Gesso Romagnola. *Memorie dell'Istituto Italiano di Speleologia*, **2**(26), pp. 81-101.

Table 1. U-Th radiometric dating results. Mass of samples, ^{238}U content, the uranium and thorium isotope activity ratios, and the corrected ages are provided. Uncertainties are expressed in 2σ notation. Ages are calculated using equation 1 of Hellstrom (2006) and the U and Th decay constants of Cheng et al, (2013). The raw ages were corrected using an initial $^{230}Th/^{232}Th$ activity ratio of 1.5±1.5.

Cave system	Cave	Sample ID	Mass (g)	^{238}U (ng/g)	$(^{230}Th/^{238}U)_A$ ± 2σ	$(^{234}U/^{238}U)_A$ ± 2σ	$(^{232}Th/^{238}U)_A$ ± 2σ	$(^{230}Th/^{232}Th)_A$	Corrected Age (ka) ± 2σ
Monte Tondo - Re Tiberio	Abisso Mezzano	RT-AI r	0.037	1483	0.6542 ± 0.0049	0.946 ± 0.004	0.000454 ± 0.000001	1440	130.58 ± 2.39
		RT-A1 bis	0.015	848	0.6541 ± 0.0043	0.945 ± 0.002	0.000657 ± 0.000006	995	131.10 ± 1.87
		RT-A1	0.106	1023	0.6558 ± 0.0012	0.945 ± 0.002	0.000848 ± 0.000007	774	131.74 ± 0.75
		RT 2015 1	0.020	1554	0.6490 ± 0.0035	0.944 ± 0.002	0.000402 ± 0.000003	1616	129.04 ± 1.53
		RT 2015 5	0.019	1656	0.6572 ± 0.0039	0.956 ± 0.002	0.000607 ± 0.000003	1082	128.67 ± 1.65
		RT-B1	0.009	934	0.6541 ± 0.0044	0.956 ± 0.003	0.000239 ± 0.000005	2733	127.57 ± 1.83
		RT 2015 7	0.019	1623	0.6510 ± 0.0028	0.957 ± 0.003	0.000730 ± 0.000004	892	125.77 ± 1.28
		RT-B I	0.010	1797	0.6479 ± 0.0052	0.952 ± 0.008	0.000125 ± 0.000001	5174	126.24 ± 3.20
		RT-B2	0.008	1068	0.6541 ± 0.0039	0.962 ± 0.003	0.000517 ± 0.000006	1266	125.87 ± 1.64
		RT-C1	0.010	1004	0.6562 ± 0.0046	0.965 ± 0.003	0.000599 ± 0.000007	1095	125.58 ± 1.85
		RT-CI	0.012	1748	0.6498 ± 0.0055	0.958 ± 0.002	0.000075 ± 0.000002	8677	125.35 ± 2.11
		RT-C m1	0.013	3127	0.6472 ± 0.0025	0.957 ± 0.002	0.000098 ± 0.000001	6606	124.95 ± 1.08
		RT-C m2	0.017	1619	0.6422 ± 0.0020	0.949 ± 0.002	0.000295 ± 0.000003	2176	125.14 ± 0.91
		RT-CII	0.012	1669	0.6389 ± 0.0053	0.951 ± 0.002	0.000250 ± 0.000003	2552	123.45 ± 2.02
		RT 2015 10	0.020	1696	0.6508 ± 0.0032	0.963 ± 0.002	0.000146 ± 0.000001	4448	124.36 ± 1.32
		RT-C2	0.015	972	0.6450 ± 0.0028	0.953 ± 0.002	0.000215 ± 0.000003	3004	125.17 ± 1.23
		RT-DI	0.033	1764	0.6461 ± 0.0049	0.955 ± 0.001	0.000682 ± 0.000003	948	124.74 ± 1.85
		RT-D III	0.050	1899	0.6484 ± 0.0048	0.961 ± 0.003	0.000684 ± 0.000003	948	123.94 ± 1.94
	3 Anelli	3A	0.014	2970	0.5932 ± 0.0025	0.946 ± 0.002	0.002052 ± 0.000027	289	108.86 ± 0.98
		3A-2016-2	0.045	534	0.6016 ± 0.0024	0.960 ± 0.002	0.005345 ± 0.000025	113	107.69 ± 1.28
		3A-t	0.020	1157	0.6223 ± 0.0037	0.968 ± 0.003	0.038551 ± 0.000421	16	106.29 ± 7.23
	Abisso 50	A501	0.008	1681	0.5176 ± 0.0025	0.970 ± 0.002	0.033461 ± 0.000349	15	77.89 ± 6.06
		A502	0.011	1867	0.4843 ± 0.0024	0.965 ± 0.002	0.002576 ± 0.000037	188	76.10 ± 0.75
		A503	0.010	955	0.4829 ± 0.0024	0.975 ± 0.002	0.001806 ± 0.000019	267	74.69 ± 0.68
	Pozzo Pollini	D3	0.100	513	0.5378 ± 0.0021	0.973 ± 0.002	0.002398 ± 0.000013	224	87.80 ± 0.70
		PP	0.015	295	0.5207 ± 0.0045	0.976 ± 0.003	0.002766 ± 0.000019	188	83.14 ± 1.24
		PP1	0.009	795	0.5201 ± 0.0029	0.970 ± 0.002	0.018004 ± 0.000116	29	81.18 ± 3.23
		D2	0.100	652	0.4886 ± 0.0009	0.950 ± 0.001	0.008241 ± 0.000022	59	77.90 ± 1.40
		D4	0.100	670	0.4912 ± 0.0013	0.957 ± 0.001	0.008062 ± 0.000030	61	77.70 ± 1.40
		PP2	0.017	1165	0.4859 ± 0.0028	0.968 ± 0.002	0.007278 ± 0.000078	67	75.21 ± 1.44
	Grotta Oliver	GO1	0.012	1217	0.0921 ± 0.0009	0.949 ± 0.002	0.023011 ± 0.000284	4	7.10 ± 4.10
		GO2	0.010	924	0.0962 ± 0.0007	0.943 ± 0.002	0.026957 ± 0.000186	4	6.96 ± 4.92
		GO-2016-2	0.044	1205	0.0670 ± 0.0004	0.939 ± 0.002	0.017181 ± 0.000321	4	5.03 ± 3.09
	Galleria Principale	RTy 1	0.047	1511	0.0052 ± 0.0002	0.960 ± 0.001	0.000451 ± 0.000008	12	0.52 ± 0.08
		RTy 2	0.045	1432	0.0035 ± 0.0002	0.960 ± 0.001	0.000613 ± 0.000014	6	0.29 ± 0.11
		RTy 3	0.051	1548	0.0042 ± 0.0001	0.982 ± 0.002	0.002122 ± 0.000050	2	0.11 ± 0.36
Spipola - Acquafredda	Spipola	Spd-2016-1	0.047	924	1.0480 ± 0.0042	1.126 ± 0.002	0.000147 ± 0.000002	7124	253.90 ± 4.41
		SpD-E	0.120	586	0.9303 ± 0.0097	1.026 ± 0.009	0.000416 ± 0.000004	2238	252.10 ± 14.77
		SpD-D	0.118	442	0.9061 ± 0.0104	1.009 ± 0.010	0.002357 ± 0.000026	384	246.63 ± 16.16
		SpD-C	0.049	1003	1.0197 ± 0.0064	1.112 ± 0.004	0.000020 ± 0.000001	50924	243.58 ± 6.52
		SpD-B	0.051	3052	1.0215 ± 0.0051	1.111 ± 0.004	0.000004 ± 0.000000	277192	245.55 ± 5.64
		SpD-A	0.050	1971	1.1318 ± 0.0055	1.207 ± 0.004	0.000465 ± 0.000009	2432	246.34 ± 5.31
		SpD b	0.063	429	0.9245 ± 0.0035	1.028 ± 0.002	0.000264 ± 0.000002	3506	243.53 ± 3.97
		Spd-2016-2	0.048	484	0.8964 ± 0.0035	1.007 ± 0.002	0.002002 ± 0.000039	448	239.34 ± 4.30
		Sp1-b	0.038	736	0.0170 ± 0.0004	1.029 ± 0.003	0.007400 ± 0.000186	2	0.63 ± 1.19
		Sp1-t	0.034	731	0.0071 ± 0.0002	1.024 ± 0.003	0.003287 ± 0.000071	2	0.23 ± 0.53
		SpS-b	0.044	1012	0.0143 ± 0.0003	1.045 ± 0.002	0.001267 ± 0.000025	11	1.30 ± 0.20
		SpS-t	0.045	1062	0.0027 ± 0.0002	1.031 ± 0.002	0.000901 ± 0.000015	3	0.14 ± 0.14
Castelnuovo	Peroni	P2-b	0.039	989	0.0818 ± 0.0007	0.984 ± 0.003	0.009378 ± 0.000174	9	7.89 ± 1.58
		P2-t	0.036	1120	0.0389 ± 0.0004	1.048 ± 0.003	0.000289 ± 0.000005	135	4.08 ± 0.06
		P3-B	0.035	1435	0.0479 ± 0.0009	1.014 ± 0.002	0.000412 ± 0.000011	116	5.22 ± 0.12
		P3-T	0.044	1368	0.0246 ± 0.0005	1.057 ± 0.002	0.000071 ± 0.000001	347	2.56 ± 0.05
	Mornig	MOR2-b	0.020	1314	0.0424 ± 0.0006	0.880 ± 0.002	0.012795 ± 0.000034	3	2.99 ± 2.44
		MOR2-t	0.021	2313	0.0218 ± 0.0003	0.857 ± 0.003	0.001254 ± 0.000005	17	2.57 ± 0.24
Stella - Rio Basino	Rio Basino	RBT-b	0.049	1076	0.0588 ± 0.0005	0.893 ± 0.003	0.013927 ± 0.000202	4	4.84 ± 2.64
		RBT-t	0.052	1102	0.0432 ± 0.0005	0.887 ± 0.003	0.008033 ± 0.000094	5	3.95 ± 1.51
		RB3-b	0.050	511	0.0252 ± 0.0005	0.937 ± 0.003	0.004679 ± 0.000060	5	2.15 ± 0.83
		RB3-t	0.050	492	0.0089 ± 0.0004	0.950 ± 0.003	0.003228 ± 0.000060	3	0.47 ± 0.56
		RB1-b	0.034	569	0.0612 ± 0.0013	0.935 ± 0.002	0.011802 ± 0.000275	5	5.29 ± 2.11
		RB1-t	0.042	494	0.0282 ± 0.0008	0.953 ± 0.002	0.010104 ± 0.000227	3	1.53 ± 1.77
Monte Mauro	Monte Mauro	MM2-b	0.039	731	0.9225 ± 0.0042	0.981 ± 0.003	0.019454 ± 0.000541	47	316.17 ± 12.65
		MM2-t	0.034	1367	0.8783 ± 0.0031	0.990 ± 0.003	0.001359 ± 0.000028	646	239.98 ± 4.46
		MM4 b	0.021	556	0.9782 ± 0.0062	0.994 ± 0.003	0.001776 ± 0.000010	551	468.00 +130/-42
		MM4 t	0.023	393	0.9375 ± 0.0060	0.995 ± 0.003	0.002130 ± 0.000009	440	313.44 ± 14.27
	Banditi	BA 1.1	0.050	1071	0.9988 ± 0.0051	0.998 ± 0.004	0.111054 ± 0.000331	9	> 580 ± -
		BA 2.1	0.050	804	0.9569 ± 0.0045	0.991 ± 0.004	0.001508 ± 0.000023	635	378.00 +29/-20
		BA_BIG_1	0.075	1837	0.6804 ± 0.0026	0.976 ± 0.004	0.000010 ± 0.000000	69553	131.29 ± 1.46
		BA_BIG_2	0.069	886	0.6776 ± 0.0030	0.987 ± 0.003	0.000011 ± 0.000001	62589	127.07 ± 1.40
		BA_BIG_3	0.066	706	0.6563 ± 0.0029	0.990 ± 0.003	0.000039 ± 0.000001	16700	119.01 ± 1.26
		BA_BIG_4	0.070	979	0.6363 ± 0.0026	0.990 ± 0.003	0.000462 ± 0.000007	1377	112.36 ± 1.09

Drysdale RN, Hellstrom JC, Zanchetta G, Fallick AE, Sanchez Goni MF, Couchoud I, McDonald J, Maas R, Lohmann G, Isola I, 2009. Evidence for obliquity forcing of glacial Termination II. Science, 325(5947), 1527-1531.

Drysdale RN, Bence TB, Hellstrom JC, Couchoud I, Greig A, Bajo P, Zanchetta G, Isola I, Spötl C, Baneschi I, Regattieri E, Woodhead JD, 2012. Precise microsampling of poorly laminated speleothems for U-series dating. *Quaternary Geochronology*, **14**, 38-47.

Falgueres C, 2003. ESR dating and the human evolution: Contribution to the chronology of the earliest humans in Europe. *Quaternary Science Reviews*, **22**, 1345–1351.

Forti P, Chiesi M, 2001. Idrogeologia, idrodinamica e meteorologia ipogea dei Gessi di Albinea, con particolare riguardo al Sistema carsico afferente alla Tana della Mussina di Borzano (ER-RE 2) (Albinea-Reggio Emilia). *Memorie dell'Istituto Italiano di Speleologia*, **2**(11), 115-139.

Forti P, 2003. I sistemi carsici. In: A Biancotti and M Motta (Eds.). Risposta dei processi geomorfologici alle variazioni ambientali, Briganti, Genova, pp. 246-251.

Hellstrom J, 2003. Rapid and accurate U/Th dating using parallel ion-counting multi-collector ICP-MS. *Journal of Analytical Atomic Spectrometry*, **18**, 1346-1351.

Hellstrom J, 2006. U-Th dating of speleothems with high initial 230Th using stratigraphical constraint. *Quaternary Geochronology*, **1**(4): 289-295.

Klimchouk AB, 2000. Speleogenesis in non carbonate lithologies. In: AB Klimchouk, DC Ford, AN Palmer and W Dreybrodt (Eds.). *Speleogenesis, evolution of karst aquifers*. National Speleological Society, Huntsville, pp. 430-442.

Lisiecki LE, Raymo ME, 2005. A Pliocene-Pleistocene stack of 57 globally distributed benthic $\delta^{18}O$ records. *Paleoceanography*, **20**(1), 1-17.

Lugli S, Manzi V, Roveri M, Scheiber BC, 2010. The Primary Lower Gypsum in the Mediterranean: a new facies interpretation for the first stage of the Messinian salinity crisis. *Palaeogeography, Palaeoclimatology, Palaeoecology*, **297**(1), 83-99.

Miari M, 2007. L'eneolitico. In: C Guarnieri (Eds.). *Archeologia dell'Apennino romagnolo: il territorio di Riolo Terme, Imola*, pp. 30-33.

Muttoni G, Scardia G, Kent DV, Morsiani E, Tremolada F, Cremaschi M, Peretto C, 2011. First dated human occupation of Italy at ~0.85 Ma during the late Early Pleistocene climate transition. *Earth and Planetary Science Letters*, **307**(3-4), 241-252.

Negrini C, 2007. Re Tiberio. In: C Guarnieri (Eds.). *Archeologia dell'Apennino romagnolo: il territorio di Riolo Terme, Imola*, pp. 51-52.

Pasini G, 1969. Fauna a mammiferi del Pleistocene superiore in un paleoinghiottitoio carsico presso Monte Croara (Bologna). Le Grotte d'Italia, **4**(4), 1-46.

Pasini G, 2012. Speleogenesis of the "Buco dei Vinchi" inactive swallow hole (Monte Croara karst sub-area, Bologna, Italy), an outstanding example of antigravitative erosion (or "paragenesis") in selenitic gypsum. An outline of the "post-antigravitative erosion". *Acta Carsologica*, **41**(1), 15-34.

Picotti V, Pazzaglia FJ, 2008. A new active tectonic model for the construction of the Northern Apennines mountain front near Bologna (Italy). *Journal of Geophysical Research*, **113**, B08412.

Plan L, Tschegg C, De Waele J, Spötl C, 2012. Corrosion morphology and cave wall alteration in an Alpine sulfuric acid cave (Kraushohle, Austria). *Geomorphology*, **169**, 45-54.

Polyak VJ, McIntosh WC, Güven N, Provencio P, 1998. Age and origin of Carlsbad Cavern and related caves from $^{40}Ar/^{39}Ar$ of Alunite. *Science*, **279**(5358), 1919-1922.

Polyak VJ, Provencio P, Asmerom Y, 2016. U-Pb dating of speleogenetic dolomite: A new sulfuric acid speleogenesis chronometer. *International Journal of Speleology*, **45**(2), 103-109.

Richards DA and Dorale JA, 2003. Uranium-series chronology and environmental applications of speleothems. *Reviews in Mineralogy and Geochemistry*, **52**(1), 407-460.

Sasowsky ID, 1998. Determining the age of what is not there. *Science*, **279**(5358), 1874.

Vai GB, Martini IP, 2001. *Anatomy of an orogen: the Apennines and adjacent Mediterranean*. Kluwer Academic Publishers, Dordrecht, Netherlands, pp. 631.

Wegmann KW, Pazzaglia FJ, 2009. Late Quaternary fluvial terraces of the Romagna and Marche Apennines, Italy: climatic, lithologic, and tectonic controls on terrace genesis in an active orogen. *Quaternary Science Reviews*, **28**(1), 137-165.